Effect of oxygen partial pressure on the local structure and magnetic properties of Co-doped ZnO films

2008 J. Phys.: Condens. Matter 20 025208

(http://iopscience.iop.org/0953-8984/20/2/025208)

J. Phys.: Condens. Matter **20** (2008) 025208 (5pp) doi:10.1088/0953-8984/20/02/025208

Effect of oxygen partial pressure on the local structure and magnetic properties of Co-doped ZnO films

Xue-Chao Liu[1,2], Er-Wei Shi[1], Zhi-Zhan Chen[1,5], Bo-Yuan Chen[1,2], Tao Zhang[1], Li-Xin Song[1], Ke-Jin Zhou[3], Ming-Qi Cui[3], Wen-Sheng Yan[4], Zhi Xie[4], Bo He[4] and Shi-Qiang Wei[4]

[1] Shanghai Institute of Ceramics, Chinese Academy of Sciences, Shanghai 200050, People's Republic of China
[2] Graduate School of the Chinese Academy of Sciences, Beijing 100049, People's Republic of China
[3] Beijing Synchrotron Radiation Facility, Institute of High Energy Physics, Beijing 100049, People's Republic of China
[4] National Synchrotron Radiation Laboratory, University of Science and Technology of China, Hefei 230029, People's Republic of China

E-mail: zzchen@mail.sic.ac.cn

Received 12 July 2007, in final form 10 October 2007
Published 6 December 2007
Online at stacks.iop.org/JPhysCM/20/025208

Abstract

$Zn_{0.95}Co_{0.05}O$ films were prepared under different oxygen partial pressures (P_{O_2}) by inductively coupled plasma enhanced physical vapor deposition. The effect of P_{O_2} on the local structure and magnetic properties was investigated. The x-ray absorption spectroscopy at the Co K-edge, Co L-edge, and O K-edge revealed that the main defects were oxygen vacancies when the films were deposited under very low P_{O_2}. The change from room-temperature ferromagnetism to paramagnetism was observed with increasing P_{O_2}. It was experimentally demonstrated that the oxygen vacancy defect is absolutely necessary to induce ferromagnetic couplings in Co-doped ZnO films.

1. Introduction

Diluted magnetic semiconductors (DMSs) are attracting intense interest for potential applications in new spintronic devices. Transition metal (TM) doped II–VI or III–V semiconductors are the most frequently studied systems, particularly Co- or Mn-doped ZnO where room-temperature ferromagnetism is theoretically predicted by Sato and Dietl [1, 2]. Experimental investigations on Co-doped ZnO show diverse magnetic properties, ranging from paramagnetic, spin-glass, and antiferromagnetic behavior to ferromagnetism below or even at high temperature [3–7]. In addition, the observed ferromagnetism is still under debate. It might originate from the formation of Co-metal clusters or secondary cobalt oxide phases [8]. Quite similar situations exist in other TM-doped ZnO systems [9–11]. It is significant to investigate the local structure of the doped magnetic ions. Recently, Coey *et al* proposed that ferromagnetic coupling in oxide-based DMSs was mediated by shallow donor electrons forming bound magnetic polarons (BMP) [12]. The theory gives a clear magnetic phase diagram, including regions of ferromagnetism, paramagnetism, spin-glass, and antiferromagnetism. In ZnO, the most common donors are native defects, particularly oxygen vacancies (V_O) and interstitial Zn (Zn_i). They can be easily generated during film growth processes owing to the vacuum environment. Theoretical and experimental studies revealed that the native defects could cause a marked change in the band structure and make a significant contribution to the ferromagnetic exchange in Co-doped TiO_2 [13]. The effect of annealing treatment on the magnetic properties has been investigated in Mn- and Co-doped ZnO films [14, 15]. However, it is difficult to measure V_O and Zn_i directly. A way to identify the kind of defect is x-ray absorption spectroscopy (XAS). It was proposed that x-ray absorption near-edge structure spectroscopy (XANES), with its advantage

[5] Author to whom any correspondence should be addressed.

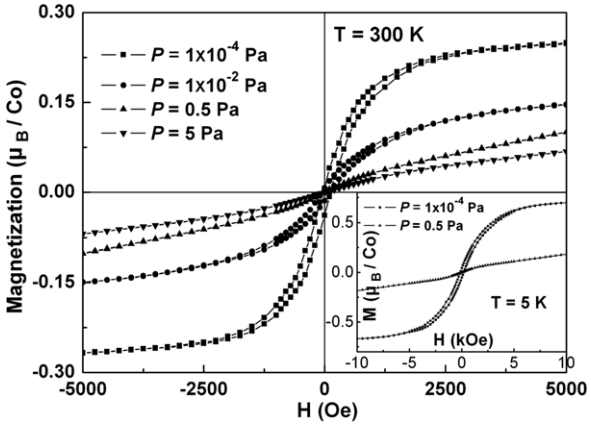

Figure 1. Magnetization hysteresis curves of $Zn_{0.95}Co_{0.05}O$ films deposited under different P_{O_2}. The inset shows hysteresis curves of $P_{O_2} = 1 \times 10^{-4}$ and $P = 0.5$ Pa samples at 5 K.

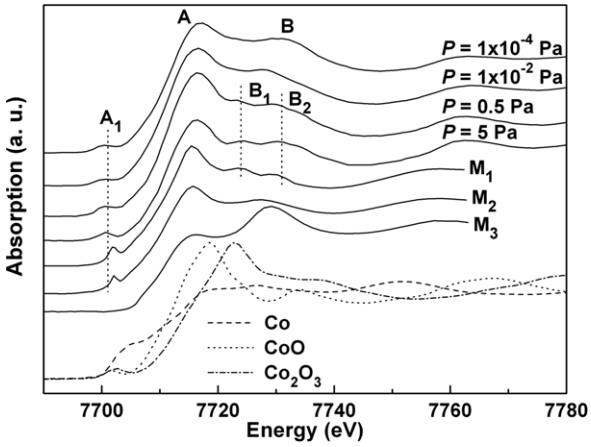

Figure 2. Co K-edge XANES spectra of $Zn_{0.95}Co_{0.05}O$ films and reference samples of Co, CoO, and Co_2O_3. The theoretically calculated XANES spectra of three different structural models (M_1, M_2, and M_3) were included to compare with experimental results.

of distinguishing the local coordination geometry and the electronic structure surrounding a special atom even in a diluted content, would be sensitive to the formation of native defects and could provide qualitative information by analyzing the change in absorption features [16]. In this paper, several $Zn_{0.95}Co_{0.05}O$ films were prepared under different oxygen partial pressures (P_{O_2}). The XANES measurement was carried out to investigate the local structure and native defects. The purpose is to reveal the correlation between the defect and magnetic properties.

2. Experiment details

The Co-doped ZnO films were deposited on Si(100) and quartz glass (for Hall measurement) substrates by inductively coupled plasma enhanced physical vapor deposition (ICP-PVD). The ICP-PVD with a magnetic confinement system and details of the preparation procedure have been described elsewhere [17]. In order to investigate the effect of P_{O_2} on the magnetic properties, the Co-doped ZnO films were deposited under different P_{O_2} (labeled as $P = {}^{**}$ Pa in the following figures). Samples studied here were all *c*-axis orientated. No detectable phases corresponding to cobalt oxides or Co clusters were found by x-ray diffraction and high resolution transmission electron microscopy. Rutherford backscattering spectroscopy was used to investigate the composition and in-depth distribution of the Co elements. The films were homogeneous with wurtzite structure and the doped Co content was estimated to be about 5.5 at.%. The above quality characterizations were described elsewhere [17]. Four-point Van der Pauw Hall measurements (LakeShore Hall measurement system, 7704A) were carried out to investigate the electrical properties at room temperature. The magnetic properties were performed using a superconducting quantum interference device (SQUID, MPMS XL-7). The Co L-edge XAS spectra were performed on the BL-2C beamline of Photon Factory (PF) in Japan. They were measured in the total electron-yield model. The Co K-edge XAS were performed on the U7c beamline at the National Synchrotron Radiation Laboratory (NSRL) in China. They were measured in the total fluorescence-yield model and a seven-element pixel high purity Ge solid-state detector was used to collect the fluorescence signal.

3. Results and discussion

The as-deposited $Zn_{0.95}Co_{0.05}O$ films show completely different magnetic behavior, as shown in figure 1. Room-temperature hysteresis curves are observed when it was deposited in a high vacuum environment ($P_{O_2} = 1 \times 10^{-4}$ Pa, deposited without oxygen plasma). The saturation magnetization (M_s) and coercivity (H_c) are 0.25 μ_B/Co and ~100 Oe, respectively. For $P_{O_2} = 1 \times 10^{-2}$ Pa sample, although the M_s (0.15 μ_B/Co) and H_c (85 Oe) decrease slightly, ferromagnetic behavior is still obvious. However, the hysteresis curve disappears when P_{O_2} was increased to above 0.5 Pa. The hysteresis loop does not appear even at a low temperature of 5 K ($P_{O_2} = 0.5$ Pa) as shown in the inset of figure 1. For $P_{O_2} = 0.5$ and 5 Pa samples, the M–H curves exhibit zero coercivity and almost linear behavior except for small fields. Therefore, the dominant magnetic interactions in the films are antiferromagnetic exchange. It should be emphasized that slight ferromagnetic exchange could not be excluded due to the low field non-linear behavior. Experimentally, the P_{O_2} plays an important role in the magnetic properties. Similar results have been found in other oxide DMSs such as Mn-doped ZnO, Co-doped TiO_2, and In_2O_3, etc [14, 18, 19].

Figure 2 shows the XANES spectra of $Zn_{0.95}Co_{0.05}O$ films at the Co K-edge. The spectra of Co, CoO, and Co_2O_3 are also provided as reference. The XANES absorption edge moves to lower energy as the effective valency decreases [20]. The absorption edges of Co, CoO, and Co_2O_3 are 7707, 7711, and 7714 eV, respectively. It is 7710–7711 eV for the $Zn_{0.95}Co_{0.05}O$ samples. It can be seen that the absorption edge of $Zn_{0.95}Co_{0.05}O$ films have close proximity to that of CoO, in marked contrast with those characteristics of Co and Co_2O_3. This reveals that the Co ions in $Zn_{0.95}Co_{0.05}O$ films

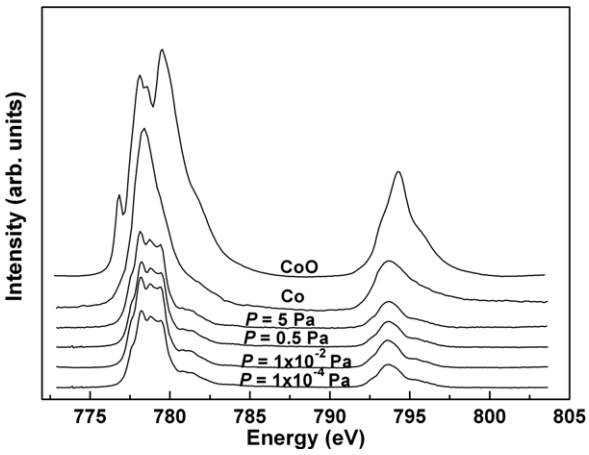

Figure 3. Co 2p XAS spectra of $Zn_{0.95}Co_{0.05}O$ films deposited under varying P_{O_2} and CoO and Co.

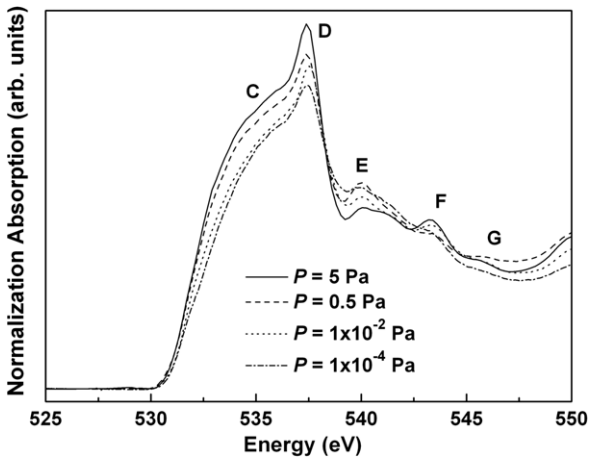

Figure 4. O K-edge XANES spectra of $P_{O_2} = 1 \times 10^{-4}$, $P_{O_2} = 1 \times 10^{-2}$, $P_{O_2} = 0.5$, and $P_{O_2} = 5$ Pa samples.

are in the +2 state. All of the $Zn_{0.95}Co_{0.05}O$ films show two main peaks (A and B) located at similar positions. An obvious peak (labeled as A_1) appears in the pre-edge region. When the $Zn_{0.95}Co_{0.05}O$ films were deposited under high P_{O_2}, the peak B splits into two small peaks (labeled as B_1 and B_2). Generally, peak A_1 is known as being characteristic of transition metals and is usually assigned to a 1s–3d transition [21]. The Co ions are located in a tetrahedral environment when Co^{2+} substitutes for Zn^{2+} in ZnO. This is a non-centrosymmetric configuration. The quadrupole 1s–3d transition is negligible in this case. The 3d–4p intra-atomic Co is possible and the Co 4p is hybridized to the Co 3d states. Thus the pre-edge peak A_1 is due to the dipole 1s–4p transitions in the Co-doped ZnO samples [21, 22]. The feature change in peak B is usually attributed to an oxygen vacancy. We investigate the effect of an oxygen vacancy by calculating the Co K-edge XANES. The simulations were calculated by the real-space multiple-scattering approach using FEFF 8.2 [23], which takes account of three structural models. In the first model (M_1), a Co atom substitutes for a Zn atom in the ZnO matrix without any V_O and Zn_i. In the second model (M_2), a Co atom substitutes for a Zn atom with one V_O in the first coordination shell. In the third model (M_3), a Co atom substitutes for a Zn atom with one Zn_i in the neighboring and possible interstitial site. The inputted structural parameters and geometrical configurations were fully optimized using the conjugate gradient technique and projector augmented plane wave method. The relaxed angle of Co–O–Zn (θ) and the bond length of Co–O (d_{Co-O}) and Co–Zn (d_{Co-Zn}) are listed in table 1 in order to compare with the original structure after introducing the oxygen vacancy. The d_{Co-O}, d_{Co-Zn} and θ of M_1 model (before optimizing) is 1.973 Å, 3.250 Å, and 109.53°, respectively. They decrease slightly to 1.922 Å, 3.208 Å, and 106.78° after relaxing the M_1 model. In the M_2 model, one oxygen atom was removed from the nearest Co atoms, so there are only three O atoms surrounding the doped Co atoms. It is difficult to measure the angle of Co=V_O=Zn, since no O atom is on the lattice site. The Co=O=Zn angle which is neighboring the oxygen vacancy was measured. It can be seen that the d_{Co-O} and d_{Co-Zn} are obviously shortened. The neighboring Co=O=Zn angle decreases to 101.31°. It can be clearly seen that the calculated XANES spectra of M_1 show two obvious splitting peak B_1 and B_2, which is in reasonable agreement with the experimental spectra of $P_{O_2} = 0.5$ and 5 Pa samples. The XANES spectra change obviously with introducing V_O and Zn_i defects. The peaks B_1 and B_2 change to one smooth peak B for M_2, which is consistent with the main features of $P_{O_2} = 1 \times 10^{-4}$ and $P_{O_2} = 1 \times 10^{-2}$ Pa samples. The change in the post-edge region may be caused by the shortening of the d_{Co-O} and d_{Co-Zn} [24]. For calculated M_3 spectrum, the intensity of peak A decreases obviously, while the intensity of peak B is enhanced dramatically. The calculated results indicate that the main donor defect is V_O when the films are deposited under very low P_{O_2}. The V_O defect could be partially eliminated by increasing P_{O_2}. Hsu *et al* obtained similar results in calculating Zn K-edge of ZnO with some oxygen atoms removed [15]. Figure 3 compares the Co $L_{2,3}$ edge XAS spectra of $Zn_{0.95}Co_{0.05}O$ films with those of CoO and Co. The peak positions and the line shape of the Co $L_{2,3}$ edge XAS spectrum depend on the local electronic structure, providing information on the valence state and the ground-state symmetry of the Co ions. The Co L-edge absorption edges correspond to transitions from the $2p_{1/2}$ and $2p_{3/2}$ states to the continuum of empty states. The Co $2p_{3/2}$ and $2p_{1/2}$ are located around 778 and 794 eV, respectively. The large energy separation is due to spin–orbit splitting of the 2p core–hole [25]. The multiplet features resulting from Coulomb and exchange interactions of the 2p core holes with the 3d electrons are clearly seen in all spectra [26]. The Co 2p XAS spectra of $Zn_{0.95}Co_{0.05}O$ films are almost the same as each other, while they are quite different from that of the Co metal sample. However, the XAS features of $Zn_{0.95}Co_{0.05}O$ films are similar to those of CoO except for the absence of the low energy shoulder (~776 eV). It is known that Co ions in CoO are located at the octahedron (O_h) centers, while Co ions in $Zn_{0.95}Co_{0.05}O$ are located at the tetrahedron (T_d) centers if Co ions are substituted for Zn ions [27]. The XAS results indicate that Co ions in $Zn_{0.95}Co_{0.05}O$ were in the divalent Co^{2+} valence states and the formation of the Co metal cluster in $Zn_{0.95}Co_{0.05}O$ samples could be ruled out. This is consistent with the XANES analyses. Figure 4 shows the normalized

Table 1. The values of d_{Co-O} and d_{Co-Zn} distance and Co=O=Zn angle used for XANES calculations by FEFF8.2.

Model	d_{Co-O} (Å)	d_{Co-Zn} (Å)	Co=O=Zn (deg)
Unoptimized	1.973	3.250	109.53
M_1	1.922	3.208	106.78
M_2	1.855	2.858	101.31

O K-edge XANES spectra of $Zn_{0.95}Co_{0.05}O$ films. The main features are similar to each other. The spectral features in the region between 530 and 538 eV (labeled C and D) can be attributed mainly to O 2p hybridization with highly dispersive Zn 4s state, which forms the bottom of the conduction band with a peak at ∼537 eV being due to transition to non-dispersive O $2p_\sigma$ (along the bilayer) and O $2p_\Pi$ (along the *c* axis) states [28]. The features in the region between 539 and 545 eV (labeled E, F, and G) are assigned to O 2p hybridized with Zn 4p states. It can be seen that the intensities of C and D features change slightly with decreasing the P_{O_2}. This might be due to the geometrical effect caused by the defects in the films. The variation in C and D indicates that the geometrical configurations changed slightly when the films were deposited under different P_{O_2}. In addition, there is an obvious shift in the absorption edge. The energy difference is about 0.15 eV for the onset of O K-edge XAS spectra between $P_{O_2} = 1 \times 10^{-4}$ and $P_{O_2} = 5$ Pa samples. The shift in the absorption edge may be due to the presence of V_O [26]. The presence of an oxygen vacancy affects the surrounding shell of the oxygen atoms by altering the 1s binding energies. In the XAS spectrum, the 1s–2p dipole excitation originates from the oxygen atoms, that is to say an oxygen vacancy existing in the shells can result in a shift in the absorption edge [29].

Table 2 shows the electrical properties of $Zn_{0.95}Co_{0.05}O$ films. The Hall results indicate that all of the films are n-type conductivity. The resistivity increases sharply when the P_{O_2} is increased from 1×10^{-4} to 5 Pa. Correspondingly, the electron concentration (n) is decreased sharply. For example, the n is 6.62×10^{19}, 2.11×10^{18}, 1.05×10^{15}, and 3.42×10^{14} cm^{-3} for the $P_{O_2} = 1 \times 10^{-4}$, 1×10^{-2}, 0.5 and 5 Pa samples, respectively. The decrease in electron concentration with increasing P_{O_2} indirectly reveals a remarkable reduction in the donor defects. Coey *et al* [12] proposed that ferromagnetic exchange was mediated by shallow donor electrons through forming bound magnetic polarons. The polaron percolation threshold δ_p and the cation percolation threshold x_p are two emphasized parameters. It was predicted that ferromagnetic exchange occurred when $x < x_p$ and $\delta > \delta_p$. The x_p is predicted to be 0.18 for ZnO. As Co content in our experiment was $x = 0.05$, $x < x_p$ is satisfied. δ_p can be calculated from the equation $\gamma^3\delta_p = 4.3$, where $\gamma = \varepsilon\,(m/m_e)$, m, m_e, and ε are electron mass, effective mass of the donor electrons, and ZnO dielectric constant, respectively. From $\varepsilon = 8.7$ and $m_e/m \sim 0.24$, $\delta_p = 9.0 \times 10^{-5}$ is obtained [30]. The critical concentration of the oxygen vacancies $n_\square$ was estimated to be 3.6×10^{18} cm^{-3} from $\delta_p = n_\square/n_o$, where n_o is the oxygen density (4.0×10^{22} cm^{-3}) for a close-packed oxygen lattice. Based on the XANES and Hall results, the obvious decrease in n suggests a great reduction in the donor defects, which is mainly caused by V_O due to the variation in P_{O_2} [31]. Experimentally, the antiferromagnetic coupling is dominated when n is less than 10^{18} cm^{-3}. Otherwise, the ferromagnetic coupling is predominant when n is more than 10^{18} cm^{-3}. However, the XANES could not give quantitative oxygen vacancy concentration. Since the conductivity is contributed mainly by donor defects. The electron concentration could indirectly reveal the V_O concentration. If we hypothesized that electrons were totally provided by V_O, the rough value of $n_\square$ was estimated to be of the magnitude of 10^{18} cm^{-3}, which is constituent with the value calculated by Coey's theory. This indicates that the BMP theory is valid in explaining our experimental results. It should be emphasized that the value of M_s for magnetic films is smaller than that of Co^{2+} in a tetrahedral crystal field (3.0 μ_B/Co), which suggests that only a fraction of Co polarons are ferromagnetically coupling. Coey suggested that the magnetic polarons may be in the form of antiferromagnetic pair, isolated ion, isolated polaron, and overlapping polaron. The antiferromagnetic pair, isolated Co ions, and polarons have no contribution to the macroscopical magnetism and reduce the average M_s. We experimentally demonstrated that the main defect was V_O when the films were deposited under very low P_{O_2}. The oxygen vacancy is necessary in inducing ferromagnetic couplings in Co-doped ZnO films.

Table 2. Electrical properties of the as-deposited $Zn_{0.95}Co_{0.05}O$ films at room temperature.

Samples (Pa)	Resistivity (Ω cm)	Electron density (cm^{-3})	Hall mobility (cm^2 V^{-1} s^{-1})	Type
$P_{O_2} = 1 \times 10^{-4}$	2.15×10^{-2}	4.62×10^{19}	3.57	n
$P_{O_2} = 1 \times 10^{-2}$	1.41	2.11×10^{18}	2.10	n
$P_{O_2} = 0.5$	2.71×10^{3}	1.05×10^{15}	8.55	n
$P_{O_2} = 5$	2.06×10^{4}	3.42×10^{14}	10.36	n

4. Conclusion

In summary, the $Zn_{0.95}Co_{0.05}O$ films were prepared under varying P_{O_2}. The effect of P_{O_2} on the local structure of $Zn_{0.95}Co_{0.05}O$ films was investigated by XANES at the Co K-edge, Co L-edge, and O K-edge. The XANES results indicate that Co^{2+} ions substitute for Zn^{2+} without changing the wurtzite structure. The main donor defect is V_O when the films were deposited under very low P_{O_2}. The Hall measurements indirectly reveal the variation in donor defects in the films. The V_O defect is necessary to induce ferromagnetic coupling in the Co-doped ZnO system.

Acknowledgments

This work was supported by the Shanghai Nanotechnology Promotion Center (No. 0452nm071) and National Natural Science Foundation of China (Nos 50702071 and 50772122). The XANES measurements were performed on synchrotron

radiation from beam line U7c at the National Synchrotron Radiation Laboratory in the University of Science and Technology of China. We thank Wen-Sheng Yan and Ke-Jin Zhou for analyzing and calculating the XANES data.

References

[1] Dietl T, Ohno H, Matsukura F, Cibert J and Ferrand D 2000 *Science* **287** 1019
[2] Sato K and Yoshida H K 2000 *Japan. J. Appl. Phys.* **39** L555
[3] Kim J H, Kim H, Kim D and Ihm Y E 2002 *J. Appl. Phys.* **92** 6066
[4] Lawes G, Risbud A S, Ramirez A P and Seshadri R 2005 *Phys. Rev.* B **71** 045201
[5] Bouloudenine M, Viart N, Colis S, Kortus J and Dinia A 2005 *Appl. Phys. Lett.* **87** 052501
[6] Liu X J, Song C, Zeng F and Pan F 2007 *J. Phys.: Condens. Matter* **19** 296208
[7] Tuan A C, Bryan J D, Pakhamov A B, Shutthanandan V, Thevuthasan S, McCready D E, Gaspar D, Krishnan K M, Gamelin D R and Chambers S A 2004 *Phys. Rev.* B **70** 054424
[8] Fouchet A, Prellier W and Mercey B 2006 *J. Appl. Phys.* **100** 013901
[9] Sharma P, Gupta A, Rao K V, Frank J O, Renu S, Rajeev A, Osorio J M, Johansson B and Gehring G A 2003 *Nat. Mater.* **2** 673
[10] Fukuura T, Jin Z W, Kawasaki M, Shono T, Hasegawa T, Koshihara S and Koinuma H 2001 *Appl. Phys. Lett.* **78** 958
[11] Kundaliya D C, Ogale S, Lofland S E, Dhar S, Metting C J, Shine D R, Ma Z, Varughese B, Ramanujachary K V, Salamancariba L and Venketesan T 2004 *Nat. Mater.* **3** 709
[12] Coey J M D, Venkatesan M and Fitzgerald C B 2005 *Nat. Mater.* **4** 173
[13] Jaffe J E, Droubay T C and Chambers S A 2005 *J. Appl. Phys.* **97** 073908
[14] Ramachandran S, Naryan J and Prater J T 2006 *Appl. Phys. Lett.* **88** 242503
[15] Hsu H S, Huang Y H, Liao Y F, Lin M Z, Lee C H, Lee J F, Chen S F, Lai L Y and Liu C P 2006 *Appl. Phys. Lett.* **88** 242507
[16] Kotani A and Shin S 2001 *Rev. Mod. Phys.* **73** 203
[17] Liu X C, Shi E W, Chen Z Z, Zhang H W, Song L X, Wang H and Yao S D 2006 *J. Cryst. Growth* **296** 135
[18] Manivannan A, Glaspell G, Dutta P and Seehra M S 2005 *J. Appl. Phys.* **97** 10D325
[19] Philip J, Punnoose A, Kim B I, Reddy K M, Layne S, Holmes J O, Satpati B, Leclair P R, Santos T S and Moodera J S 2006 *Nat. Mater.* **5** 298
[20] Murakami M, Matsumoto Y and Hasegawa T 2004 *J. Appl. Phys.* **95** 5330
[21] Sankar G, Sarode P R and Rao C N R 1983 *Chem. Phys.* **76** 435
[22] Sans J A, Sanchez-Royo J F, Pellicer-Porres J, Segura A, Guillotel E, Martinez-Criado G, Susini J, Munoz-Paez A and Lopez-Flores V 2007 *Superlatt. Mirostruct.* **42** 226
[23] Ankudinov A L, Bouldin C E, Rehr J J, Sims J and Hung H 2002 *Phys. Rev.* B **65** 104107
[24] Wang Q W and Liu W H 1994 *X-ray Absorption Fine Structure and its Application* (Beijing: Science Press) p 102
[25] Laan G V and Kirkman I W 1992 *J. Phys.: Condens. Matter* **4** 4189
[26] Chang G S, Kurmaev E Z, Boukhvalov D W, Finkelstein L D, Colis S, Pedersen T M, Moewes A and Dinia A 2007 *Phys. Rev.* B **75** 195215
[27] Wi S C, Kang J S, Kim J H, Cho S B, Kim B J, Yoon S and Suh B J 2004 *Appl. Phys. Lett.* **84** 4233
[28] Chiou J W, Jan J C, Tsai H M, Bao C W, Pong W F, Tsai M H, Hong I H, Klauser R, Lee J F, Wu J J and Liu S C 2004 *Appl. Phys. Lett.* **84** 3462
[29] Tuomisto F, Saarinen K, Look D C and Farlow G C 2005 *Phys. Rev.* B **72** 085206
[30] Pearton S J, Norton D P, Ip K, Heo Y W and Steiner T 2005 *Prog. Mater. Sci.* **50** 293
[31] Hsu N E, Hung W K and Chen Y F 2004 *J. Appl. Phys.* **96** 4671